DOI 10.5162/Ultrasonic2025/A8-a1

Sixty-Seven Years in Nonlinear Acousto-Optics

Laszlo Adler[1]
[1] The Ohio State University, Integrated Systems Engineering
Clearwater, Florida, United States of America

Abstract: In the late 1950s the Ultrasonic Group at Michigan State University introduced light diffraction to study distortion of ultrasonic waves in liquids under the direction of Professor Egon Hiedemann. In this paper, some results of these studies will be presented (with a detailed description of the author's measurements of B/A). The rate at which the harmonics are developed (the wave distortion is an indication of the harmonics present) during the propagation of the initially sinusoidal ultrasonic wave depends on the nonlinearity of the medium. The light which is diffracted by the distorted wave results in an asymmetric pattern contrary to Raman–Nath theoretical prediction. From the light intensity measurements due to the generated second harmonics—filtered out by a metal plate—the Nonlinearity Parameter B/A was determined. In the 1970s at the University of Tennessee, a similar filtering technique was also applied to study imaging mechanisms in the Bragg diffraction region of finite amplitude waves. Developments in studying finite amplitude standing ultrasonic waves in a liquid filled cavity will be also discussed. Using light diffraction measurements, it was observed that above a threshold amplitude, fractional harmonics of the driver transducer are also generated in addition to the generated harmonics. Some of these fractional harmonics are lower and some of them are higher frequencies than the frequency of the driver. The generation mechanism of the fractional harmonics is explained based on parametric resonance. It was recently observed that above a second threshold value of the driver's amplitude, the system undergoes chaotic behavior. Further increase of the driver's amplitude returns the system from chaos to stable oscillation.

Keywords: Nonlinear, Acousto-Optics, Subharmonics, Chaos, Liquids

Introduction and Background

Diffraction of Light by Ultrasonic Waves

Ever since it was predicted by Brillouin [1] in 1922 that light will be scattered by ultrasound in transparent materials, thousands of investigators studied the interaction of light with ultrasound. In 1932 Debye and Sears [2] in the USA and Lucas and Biquard [3] in France independently observed that when a monochromatic light beam propagates perpendicularly through an ultrasonic beam, the light will diffract into several orders (Brillouin actually predicted that the light will produce only a single order after the interaction with the ultrasound). A theoretical model was suggested by Sir Raman and Nath [4] (it is known today as Raman–Nath theory). They proposed that the ultrasonic wave behaves like a diffraction grating for the light which will produce the diffraction orders. Starting with the electromagnetic wave equation and introducing a variable refractive index for the light, they were able to predict the intensity of each order as well as the positions of the orders. The intensity of the diffracted light in the nth order is given in Eq. (1),

$$I_n = \mathrm{J}_n^2(v). \tag{1}$$

J_n is the nth order Bessel function with the argument v, which is called the Raman–Nath parameter related to the pressure of the ultrasonic wave.

$$v = \frac{2\pi\mu a}{\lambda}, \tag{2}$$

where a is the width of the sound field, λ is the wavelength of the light, and μ is the variation of the refractive index of the liquid due to the density variation caused by the ultrasonic pressure. The angle Θ of the diffracted light is given by

$$\sin(\Theta) = \frac{n\lambda}{\lambda^*} \tag{3}$$

where λ^* is the wavelength of the sound.

Diffraction of Light by Finite Amplitude Ultrasonic Waves

For higher ultrasonic frequencies the spacing between orders is larger than for the smaller ones. The intensity distribution of the diffracted light is symmetrical, i.e. the intensity of the first diffracted light to the right from the incident light is the same as to the left, because it is the square of the Bessel functions. The theory of Raman and Nath was in good agreement

DOI 10.5162/Ultrasonic2025/A8-a1

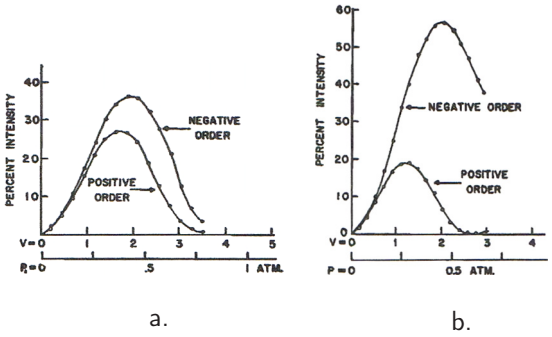

Fig. 1: Intensity of light measured in the first order for a $4\,\mathrm{MHz}$ *ultrasonic wave in water as a function of the pressure at a distance from the source: a. at* $10\,\mathrm{cm}$ *and b. at* $50\,\mathrm{cm}$.

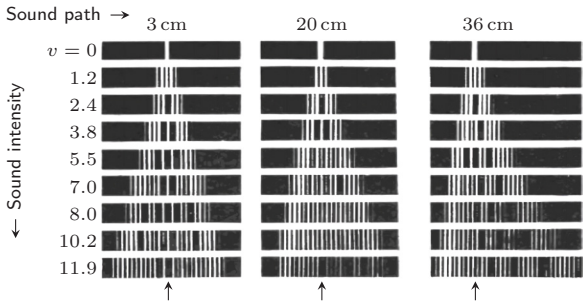

Fig. 2: Light diffraction by ultrasonic waves in water with frequency of $1.76\,\mathrm{MHz}$ *at* $3\,\mathrm{cm}$, $20\,\mathrm{cm}$, *and* $36\,\mathrm{cm}$.

with the experimental results for low-intensity ultrasound, i.e. for infinitesimally small ultrasonic amplitudes. Ken Zankel [5] observed asymmetry in the diffraction pattern. One possible explanation was the non-normal incidence of the light to the sound field. This was eliminated by proper alignment. There could have been another explanation for the asymmetry in the diffraction pattern—frequency range, width of the sound field—however it was demonstrated that the major effect of the asymmetry is due to the large amplitude of the ultrasonic waves or the so-called finite amplitude, in contrast with the infinitesimal amplitude. As a sinusoidal wave propagates with finite amplitude the ultrasonic wave form distorts due to the nonlinearity of the medium, producing harmonics, thus causing the asymmetry in the light diffraction pattern. The asymmetry in the first orders (the difference in the negative and positive order) of the measured light intensity is increasing with distance, as shown in Fig. 1, illustrating that the wave distortion increases with distance. The asymmetry in the diffraction pattern also increases with the increase of fundamental pressure as illustrated on a photograph in Fig. 2, which was taken by Mack Breazeale [6]. The asymmetry in the diffraction pattern is increasing with increasing distance of the ultrasound and with increasing sound intensity as illustrated in Fig. 2. The distortion of the ultrasonic waveform will be explained after a brief review of nonlinear acoustics which is described briefly in the next section.

Nonlinear Acoustics in Fluids

In general, a sound beam changes the wave shape as it propagates in a fluid (as well as in solids), whose pressure-density relationship does not obey Hooke's law. This means that harmonics are generated as the wave progresses. For infinitesimal amplitudes, the change in wave shape is so small that it can be neglected, however, it has to be considered for finite amplitude waves. The distortion of a finite amplitude wave is due to the nonlinear property of the medium in which the wave propagates. The positive and negative increment in pressure is impressed on the medium. The change in the volume of the mass not being equal, the volume change for positive pressure will be less than the volume change for negative pressure. Thuras, Jenkins, and O'Neil [7] in 1935 studied finite amplitude effects in gases. They have pointed out that the equation of state for adiabatic processes (such as sound propagation) shows that the linear relationship between pressure and volume does not hold and consequently leads to distortion of the wave. They derived a nonlinear wave equation and obtained an approximate solution for the generation of harmonics as a function of distance, fundamental pressure and frequency. Fox and Wallace [8] in 1959 following the same argument for liquids assumed a power series of relation between pressure and density

$$P = P_0 + A\frac{\rho - \rho_0}{\rho_0} + \frac{B}{2}\left(\frac{\rho - \rho_0}{\rho_0}\right)^2, \qquad (4)$$

where P and ρ are the instantaneous pressure and density of the liquid respectively, P_0 and ρ_0 are the pressure and density of the undisturbed liquid, and B/A is called the Nonlinearity Parameter for liquids. They derived a nonlinear wave equation for liquids, given in Eq. (5) for a one dimensional dissipationless case for the particle displacement ξ

$$\frac{\partial^2 \xi}{\partial t^2} = c^2 \frac{\partial^2 \xi}{\partial x^2} \Bigg/ \left(1 + \frac{\partial \xi}{\partial x}\right)^{(B/A+2)}, \qquad (5)$$

where ξ is the particle displacement and c is the velocity of sound in the liquid.

For infinitesimal amplitude waves the value of $\partial\xi/\partial x$ is much less than 1, and it can be neglected and Eq. (5) reduces to the linear wave equation as expected. Fox and Wallace also suggested a graphical analysis of the distorted wave. As they pointed out, the gradually steepening wave front would ultimately form a discontinuity without some stabilizing mechanism. This stabilizing mechanism is the attenuation of the ultrasound in the medium. Fox and Wallace also evaluated the Nonlinearity Parameters B/A for some liquids from compressibility data. Fubini-Ghiron [9] in 1935 used an analytical method to obtain an exact solution of the nonlinear wave equation, the paper which was published in Italian in the Alta Frequenza was not discovered before the same solutions were obtained independently by Hargrove [10] (at Michigan State University) and Keck and Bayer [11] (Brown University) in 1960. The solutions of Eq. (5) for the pressure amplitudes P_n of the nth harmonic of the distorted wave is given as,

$$P_n(k) = \frac{2P_1(0)}{nk} \mathrm{J}_n(nk), \tag{6}$$

where J_n is the nth order Bessel function, $k = x/L$, the ratio of the propagation distance x to the discontinuity distance L, that is the distance in a dissipationless liquid where the distorted wave slope will become infinite. The value of L is given by

$$L = c^3 \rho_0 \left(2 \left(\frac{B}{2A} + 1 \right) P_1(0) f \right)^{-1}, \tag{7}$$

where $P_1(0)$ is the peak acoustic pressure amplitude of the initial sinusoidal wave with frequency f.

Determination of the Nonlinearity Parameter B/A for Liquids [12]

One can calculate an expression for the amplitude of the second harmonic at any distance x from the source by expanding the Bessel function in a power series and dropping higher-order terms

$$P_2(x) = \frac{\pi}{2} \frac{B/A + 2}{\rho_0 c^3} x f P_1^2(0). \tag{8}$$

From Eq. (8), the Nonlinearity Parameter B/A is given by

$$B/A = \frac{2c^3 \rho_0}{\pi f} \frac{P_2(x)}{x P_1^2(0)} - 2. \tag{9}$$

Curves representing $P_2(x)/P_1^2(0)$ for a given medium, temperature, and frequency, and for various distances and initial pressures should extrapolate with zero slope to a common point for $xP_1(0) = 0$. The Nonlinearity Parameter B/A may then be determined from

$$B/A = \frac{2c^3 \rho_0}{\pi f} \left[\frac{P_2(x)}{x P_1^2(0)} \right]_{xP_1(0)=0} - 2. \tag{10}$$

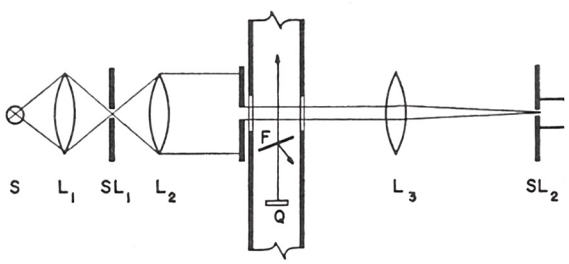

Fig. 3: Schematic diagram of the experimental arrangement.

As can be seen from Eq. (10), the amplitude of the second harmonic $P_2(x)$ and the amplitude of the fundamental $P_1(0)$ need to be measured to obtain the value of B/A for a given liquid and at a given frequency of the initial ultrasonic waves.

Experimental Arrangement and Procedure to Determine B/A

The experimental arrangement is shown schematically in Fig. 3. Light from the Hg-vapor lamp S is condensed by lens L_1 onto the source slit SL_1. The lens L_2 is adjusted by autocollimation to render the light parallel. The collimated light beam passes through a specially designed tank, and lens L_3 produces an image of the source slit SL_1 in the plane of the entrance slit SL_2 of the photomultiplier microphotometer P. A filter which passes the $5461\,$Å Hg line is located inside the photomultiplier. The transducer Q is an air-backed $1\,\mathrm{in} \times 1\,\mathrm{in}$ quartz excited at its fundamental frequency. The acoustic filter F is a stainless steel plate with a $1\,\mathrm{mm}$ thickness. When light passes through an ultrasonic wave in the liquid, various orders of diffraction are observed in the plane of the photomultiplier entrance slit. The peak change of refractive index μ is related to the peak sound pressure amplitude, a is the distance the light travels through the sound field and λ is the wavelength of light. From measurements of light intensity in the diffracted orders v may be determined from Eq. (2). To determine the pressure amplitude P from v the relationship between the change of refractive index μ and change in pressure P must be known. It is common usage to express the relationship between the change of refractive index and pressure by means of the theoretically derived expression obtained in 1880 by Lorentz–Lorenz [13]. They assumed that the molecules are optically isotropic. It is known, however, that it is not true for most liquids. In this work we used a formula obtained by Eykman [14] in 1895:

$$\mu = \frac{(\mu_0 - 1)(\mu_0 + 1.4\mu_0 + 0.4)}{\mu_0^2 + 0.8\mu_0 + 1} P, \tag{11}$$

DOI 10.5162/Ultrasonic2025/A8-a1

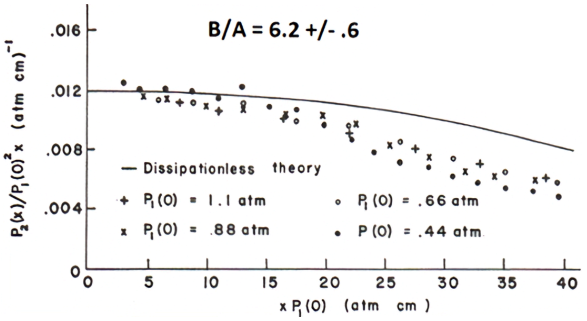

Fig. 4: Plot of reduced variables for determination of B/A in water.

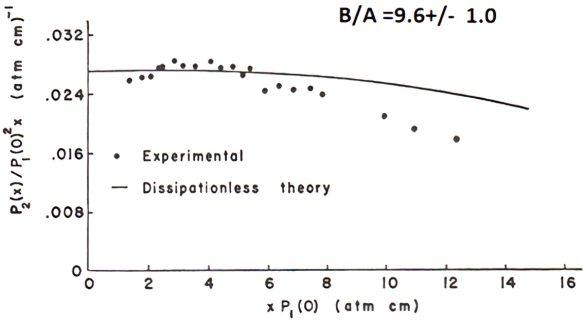

Fig. 5: Plot of reduced variables for determination of B/A in m-xylene.

where μ_0 is the refractive index of the undisturbed medium and P is the change of pressure.

Using Eq. (11) we obtain the relationship between P and v:

$$P = 0.56v/a\,\mathrm{atm} \tag{12}$$

for water and

$$P = 0.25v/a\,\mathrm{atm} \tag{13}$$

for m-xylene, where a is in cm.

Determinations of $P_1(0)$ were made from diffraction order light intensities for small sound amplitudes and near the transducer, where the waveform is undistorted (a necessary condition to use Raman–Nath theory, Eq. (1)). It was then assumed that the voltage across the transducer and $P_1(0)$ are linearly related. Values of $P_1(0)$ were obtained from the voltage across the transducer. For certain angles of incidence of the ultrasonic wave on the acoustic filter plate the fundamental component of the ultrasonic wave is reflected, and the second harmonic is transmitted [5, 15]. Using a weak ultrasonic wave with fundamental frequency corresponding to the second harmonic frequency of the finite amplitude wave to be investigated, measurements of the second harmonic component of the finite amplitude ultrasonic waves were made in water and in m-xylene for a $3.0\,\mathrm{MHz}$ fundamental frequency.

Fig. 4 shows $P_2(x)/(xP_1^2(0))$ vs. $xP_1(0)$ for water and Fig. 5 is a similar plot for m-xylene. From extrapolation of these data to $xP_1(0) = 0$ and using Eq. (10) $B/A = 6.2$ for water and $B/A = 9.6$ for m-xylene were determined. The estimated errors are within $10\,\%$.

The value of B/A for water is about $15\,\%$ higher than what is reported later. One source of error of the optical measurement is due to the conversion from refractive index variation μ to the acoustic pressure P.

Bragg Diffraction and Imaging of Light Through Finite Amplitude Ultrasonic Waves

When light interacts with an ultrasonic wave the light diffracts into several orders because the ultrasonic waves behave as a diffraction grating. This phenomenon is often referred to as Raman–Nath diffraction. In addition, there is another type of diffraction mechanism called Bragg diffraction which is more analogous to the diffraction of x-rays by a crystalline lattice. There is a region of overlap of the two mechanisms defined by the so-called Cook–Klein [16] parameter. A new means of studying Bragg diffraction was introduced by Korpel [17] in 1966, who demonstrated by using an infinitesimal ultrasonic amplitude that the first Bragg diffraction order contains an image of the ultrasonic wavefront, as well as an object placed in the ultrasonic beam. When finite amplitude ultrasonic waves are used, the problem becomes nonlinear [18]. The schematic of the experimental system is shown in Fig. 6. The RF signal is generated by a controlled oscillator. An X-cut square quartz transducer of $1\,\mathrm{in}$ in diameter was excited by using the harmonics of a $2\,\mathrm{MHz}$ fundamental frequency. The optical system consisted of a laser source and a cylindrical optical

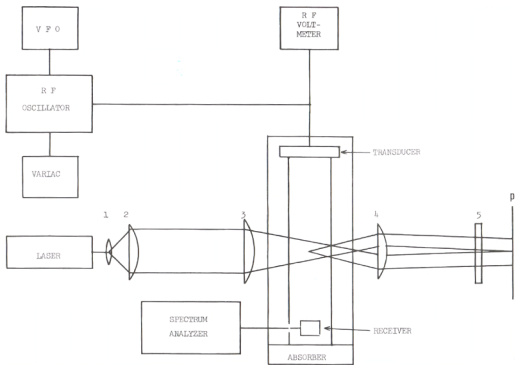

Fig. 6: Experimental system to observe Bragg imaging.

DOI 10.5162/Ultrasonic2025/A8-a1

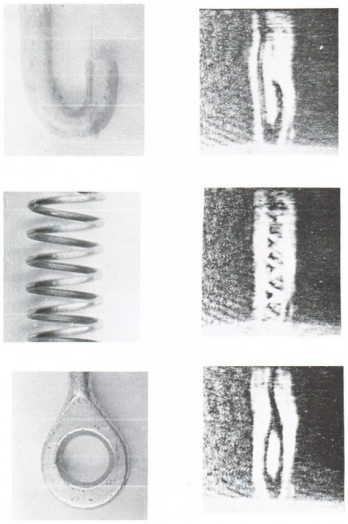

Fig. 7: Photographs of objects and their Bragg diffraction images.

system to obtain a wedge of light. This way the positive and negative Bragg diffraction orders would be observed simultaneously. Bragg imaging was obtained by placing an object to be imaged in the ultrasonic field between the transducer and the light beam. In Fig. 7 the objects and the corresponding Bragg images are shown. The images were made with an $18\,\mathrm{MHz}$ ultrasonic transducer ($2\,\mathrm{MHz}$ transducer was driven at the 9th harmonic).

As the amplitude of the ultrasonic wave increased multiple orders of Bragg diffraction are produced and multiple images of the objects were obtained, two in the second order, three in the third order as shown in Fig. 8. When finite amplitude ultrasonics was used, the ultrasonic wave got distorted and harmonics were generated. Using a transmission plate (like to measure B/A) to filter out the fundamental from the harmonics, images of double size images were obtained, since the magnification of the image is proportional to the frequency. In Fig. 9a, the double images of the hook are shown in second order. In Fig. 9b, the single image with twice the size is shown in the second order when only the second harmonics are present.

Subharmonic Generation in Water-Filled One Dimensional Cavity

While studying finite amplitude standing waves in a liquid filled cavity bounded at one end by a rigid reflector and the other end by a quartz transducer, extra orders in the diffraction pattern were observed [19, 20]. The extra orders appear only above a certain threshold voltage of the driver transducer. In Fig. 10, the diffraction pattern is shown for below the threshold value of parametric excitation in Fig. 10a, and above the threshold in Fig. 10b.

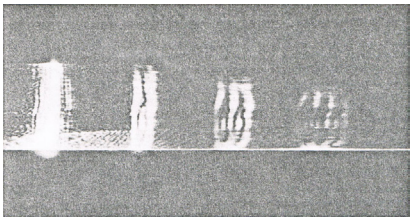

Fig. 8: Photograph of first, second and third order images of the loop.

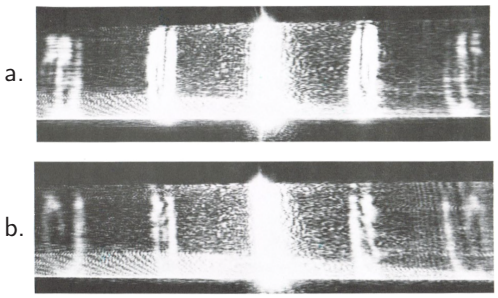

Fig. 9: Photographs of first and second order Bragg images a. without filter and b. with filter.

The extra diffraction orders shown in Fig. 10b were obtained due to the subharmonics generated at approximately half the frequency of the driver. The acoustical frequency spectrum shown on Fig. 11 corresponds to the optical diffraction pattern in Fig. 10b. It was taken by the spectrum analyzer. The driver frequency is called $2f$, which is $4\,\mathrm{MHz}$ in this case and the driver voltage is $100\,\mathrm{V}$. The other frequencies are

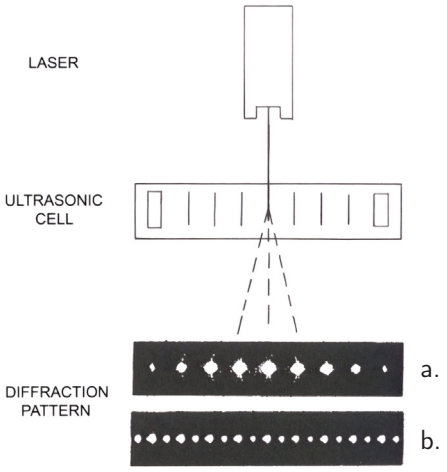

Fig. 10: Schematic diagram of the diffraction pattern below the threshold a. and above threshold b.

DOI 10.5162/Ultrasonic2025/A8-a1

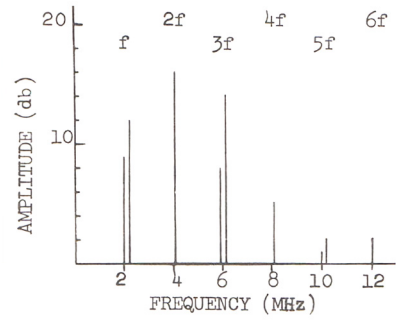

Fig. 11: Frequency spectrum at driver's voltage $100\,\mathrm{V}$.

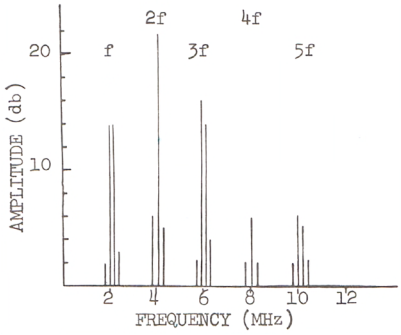

Fig. 12: Frequency spectrum at driver's voltage $200\,\mathrm{V}$.

grouped as follows: 1: $4f$, $6f$—these are the second and third harmonics of the driver. These components are present even below the threshold value of the parametric excitation and are due to the nonlinearity of the liquid. 2: The frequency pairs at f, $3f$ and $5f$, i.e. about one half, three halves and five halves the driver frequency, are sometimes called more appropriately fractional harmonics. These components are affected by the amplitude of the driver and other parameters e.g. the liquid used, geometry, the system etc.. With increased amplitude of the driver, the complexity of the spectrum increases as shown in Fig. 12 and Fig. 13, where the driver voltage increased to $200\,\mathrm{V}$ and $300\,\mathrm{V}$ respectively (it has been recognized only recently that the cascade of bifurcation leads essentially to chaos in the system, this will be discussed in the next section).

The theory to describe the generation of the subharmonics was based on a model used as a parametric system. In Fig. 14 the schematic of this system is shown. It implies that the cavity length is not constant, but it is a function of time. The variation of the cavity length is determined by the frequency as well as by the amplitude of the driver transducer. This resonant system has resonant frequencies which are themselves time dependent quantities.

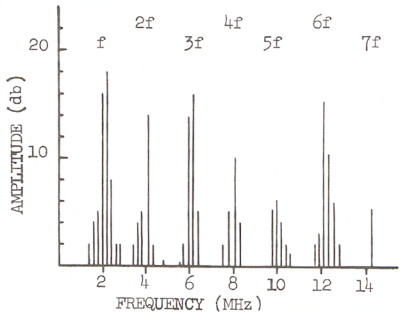

Fig. 13: Frequency spectrum at driver's voltage $300\,\mathrm{V}$.

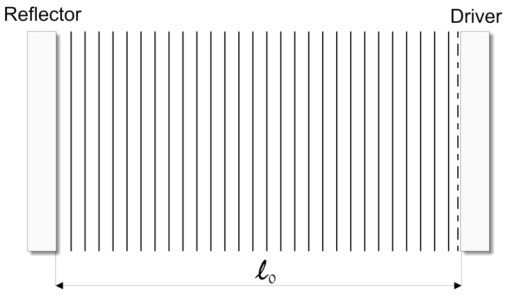

Fig. 14: Periodically varying cavity.

If the amplitude of the driver is A and the frequency is 2ω, the time dependent cavity length may be expressed as

$$l(t) = l_0(1 + h\cos(2\omega t)), \tag{14}$$

where $h = A/l_0$. The resonant frequency of the cavity takes its time dependent form

$$\omega_n(t) = \omega_n(1 + h\cos(2\omega t)). \tag{15}$$

Such vibration is not predicted by the standard normal mode solution. As a matter of fact, one cannot speak in a real sense about normal modes any more because the cavity length variation causes a fluctuation of the modes. This leads to instabilities as the source of parametric excitation of the fractional harmonics.

From the wave equation the solutions were obtained in terms of damped Mathieu functions [21] with a condition to obtain unstable solution as

$$h > c\alpha/\omega, \tag{16}$$

where c and α are the velocity and the absorption coefficient of the ultrasonic wave in the liquid. Eq. (16) relates the vibration amplitude to the other parameters of the system, and it is interpreted as the threshold condition to obtain parametric resonance. This means that parametric excitation

DOI 10.5162/Ultrasonic2025/A8-a1

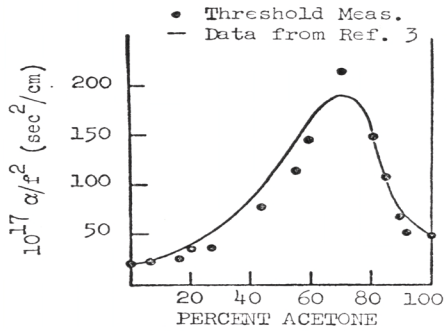

Fig. 15: Relative Absorption Coefficient as function percentage in a Water-Acetone mixture.

is a cumulative phenomenon. It is possible only if the energy input to the system, owing to a periodic variation of its resonant frequency, is greater than the energy dissipated by the system. This is the physical significance of the threshold. It was suggested to use the threshold condition in Eq. (16) to measure attenuation coefficients α for liquids [22]. In Fig. 15 the relative absorption coefficient is shown as a function of acetone concentration in water-acetone mixture as measured from the threshold of parametric excitation in the liquid mixture, and it compared very well with conventional absorption measurement.

Chaos and Beyond in a Liquid-Filled Ultrasonic Resonant System

As was pointed out in the previous section, discussing the mechanism of subharmonic generation, an increase of the driver's amplitude produces a cascade of bifurcation, see Fig. 11, 12, and 13. The problem was recently revisited with an improved experimental system shown in Fig. 16. It consists of an interferometer with optical precision controls used to adjust the positions of the piezoelectric transducer ($1\,\mathrm{MHz}$ – $10\,\mathrm{MHz}$ driven by a powerful amplifier) and a receiving transducer attached to an aligned reflector with lapped, flat, and parallel surfaces used to measure the generated frequency components in the cavity.

A visual assessment of the phenomena is obtained by passing laser light through the ultrasonic beam as indicated in Fig. 17. The laser light is diffracted into various orders n at angles given by Eq. (3).

Fig. 17 shows the diffraction patterns obtained for various transducer drive amplitudes (voltages): a. low amplitude ultrasonic waves ($5\,\mathrm{V}$); b. finite amplitude waves ($50\,\mathrm{V}$) resulting in an asymmetric diffraction pattern; and c. parametric resonance ($150\,\mathrm{V}$) producing extra diffraction orders due to the generation of the subharmonics.

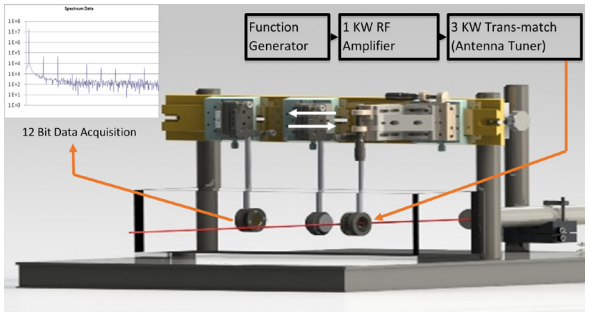

Fig. 16: Experimental system.

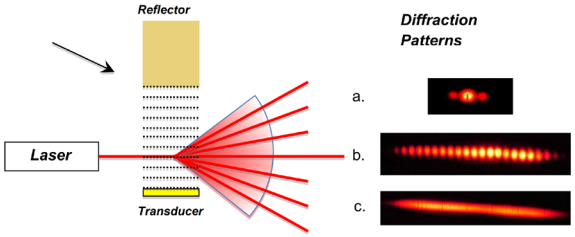

Fig. 17: Laser beam diffraction by ultrasonic wave: a. Linear Region, b. Nonlinear Region, c. Subharmonic Region.

Path to Chaos

A significantly higher transducer drive voltage ($450\,\mathrm{V}$) in the parametric resonance region leads to a cascade of bifurcations with increasing drive amplitudes that culminates in the generation of the chaotic pattern shown in Fig. 18a. Instead of distinct diffraction orders, the laser produces a smeared-out image due to the chaotic oscillations. Further increases in the transducer drive voltage (to $500\,\mathrm{V}$) lead to a second region of stability following the region of chaotic instability. The diffraction pattern in the second region of stability is shown in Fig. 18b. The pattern is similar to that of Fig. 17c, indicating the presence of stable subharmonics.

The chaotic behavior in the liquid-filled ultrasonic resonant system is generated at a second threshold (it was pointed out earlier that subharmonic generation requires a threshold power input). It is significant to notice from Fig. 18b that at an additional power level the chaos reverses into stable oscillation, i.e. beyond chaos. This observation is quite rare in chaotic systems, although some theoreticians are predicting the reversal of chaos. It should be mentioned that hysteresis is also observed when the power level changes from chaos to beyond and back to chaos. The question that remains unanswered is the physical mechanism involved when chaos is produced. One possible mechanism is "turbulence" which may take place in water at high power. Another possibility is phase transforma-

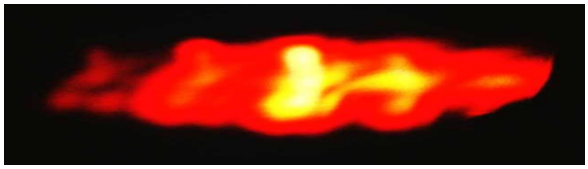

a. Chaos

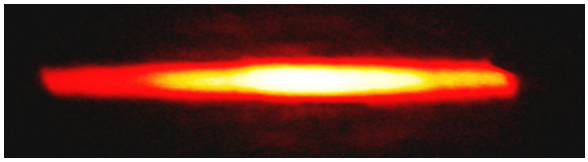

b. Beyond Chaos

Fig. 18: Laser Beam Diffraction Ultrasonic Waves: a. In the Chaotic Region ($450\,\mathrm{V}$) b. Beyond Chaotic Region ($500\,\mathrm{V}$).

tion in water, i.e. boiling, and subsequent formation of bubbles. Both of these mechanisms are examples of chaotic behavior. Additional work is required to evaluate the source of chaos in this system.

Summary

It was demonstrated that diffraction of light through ultrasonic waves with finite amplitudes provided many new observations and better understanding in nonlinear acoustics:

1. Measurements of the Nonlinearity Parameter B/A in liquids. It is important to describe the equation of state in liquids. It was found better evaluation of soft tissues.

2. Bragg Imaging with Second Harmonics. Provides an increased magnification of the images.

3. Observation of fractional harmonics in a one dimensional liquid filled ultrasonic cavity. The system was modelled as parametric resonance. The threshold condition is used to measure relative attenuation coefficient of liquids.

4. Observation of multilevel bifurcation of subharmonics, a path to chaos at a second threshold level. At an increased amplitude level the chaotic behavior reverses for stable subharmonics.

Acknowledgements

This work was partially supported by the Emeritus Academy at Ohio State University.

References

[1] L. Brillouin. "Diffusion de la lumière et des rayons X par un corps transparent homogène: Influence de l'agitation thermique". In: *Annales de Physique* 9.17 (1922), pp. 88–122. ISSN: 1286-4838. DOI: 10.1051/anphys/192209170088.

[2] P. Debye and F. W. Sears. "On the Scattering of Light by Supersonic Waves". In: *Proceedings of the National Academy of Sciences* 18.6 (June 1932), pp. 409–414. ISSN: 1091-6490. DOI: 10.1073/pnas.18.6.409.

[3] R. Lucas and P. Biquard. "Propriétés optiques des milieux solides et liquides soumis aux vibrations élastiques ultra sonores". In: *Journal de Physique et le Radium* 3.10 (1932), pp. 464–477. ISSN: 0368-3842. DOI: 10.1051/jphysrad:01932003010046400.

[4] C. V. Raman and N. S. Nagendra Nath. "The diffraction of light by high frequency sound waves: Part I." In: *Proceedings of the Indian Academy of Sciences - Section A* 2.4 (Oct. 1935), pp. 406–412. ISSN: 0973-7685. DOI: 10.1007/BF03035840.

[5] L. E. Hargrove, K. L. Zankel, and E. A. Hiedemann. "Effects of a Progressive Ultrasonic Wave on a Light Beam of Arbitrary Width". In: *The Journal of the Acoustical Society of America* 31.10 (Oct. 1959), pp. 1366–1371. ISSN: 1520-8524. DOI: 10.1121/1.1907636.

[6] M. A. Breazeale. "Experimental Studies of the "Least Stable Waveworm."" In: *The Journal of the Acoustical Society of America* 33.6 (June 1961), pp. 857–857. ISSN: 1520-8524. DOI: 10.1121/1.1936919.

[7] A. L. Thuras, R. T. Jenkins, and H. T. O'Neil. "Extraneous Frequencies Generated in Air Carrying Intense Sound Waves". In: *Bell System Technical Journal* 14.1 (Jan. 1935), pp. 159–172. ISSN: 0005-8580. DOI: 10.1002/j.1538-7305.1935.tb00688.x.

[8] F. E. Fox and W. A. Wallace. "Absorption of Finite Amplitude Sound Waves". In: *The Journal of the Acoustical Society of America* 26.6 (Nov. 1954), pp. 994–1006. ISSN: 1520-8524. DOI: 10.1121/1.1907468.

[9] E. Fubini Ghiron. "Anomalie nella propagazione di onde acustiche di grande ampiezza". In: *Alta frequenza: rivista di elettronica* 4 (1935), pp. 530–581.

[10] L. E. Hargrove. "Fourier Series for the Finite Amplitude Sound Waveform in a Dissipationless Medium". In: *The Journal of the Acoustical Society of America* 32.4 (Apr. 1960), pp. 511–512. ISSN: 0001-4966. DOI: 10.1121/1.1908127.

[11] W. Keck and R. T. Beyer. "Frequency Spectrum of Finite Amplitude Ultrasonic Waves in Liquids". In: *The Physics of Fluids* 3.3 (May 1960), pp. 346–352. ISSN: 0031-9171. DOI: 10.1063/1.1706039.

[12] L. Adler and E. A. Hiedemann. "Determination of the Nonlinearity Parameter B/A for Water and m-Xylene". In: *The Journal of the Acoustical Society of America* 34.4 (Apr. 1962), pp. 410–412. ISSN: 0001-4966. DOI: 10.1121/1.1918142.

[13] H. A. Lorentz. "Ueber die Beziehung zwischen der Fortpflanzungsgeschwindigkeit des Lichtes und der Körperdichte". In: *Annalen der Physik* 245.4 (Jan. 1880), pp. 641–665. ISSN: 1521-3889. DOI: 10.1002/andp.18802450406.

[14] M. J. F. Eykman. "Recherches réfractométriques (suite)". In: *Recueil des Travaux Chimiques des Pays-Bas* 14 (1895), p. 177. DOI: https://doi.org/10.1002/recl.18950140702.

[15] V. A. Krassilnikov, V. V. Shklovskaya-Kordy, and L. K. Zarembo. "On the Propagation of Ultrasonic Waves of Finite Amplitude in Liquids". In: *The Journal of the Acoustical Society of America* 29.5 (May 1957), pp. 642–647. ISSN: 1520-8524. DOI: 10.1121/1.1908994.

[16] W. Klein, B. Cook, and W. Mayer. "Light diffraction by ultrasonic gratings". In: *Acta Acustica united with Acustica* 15.2 (1965), pp. 67–74.

[17] A. Korpel. "Visualization of the cross section of a sound beam by Bragg diffraction of light". In: *Applied Physics Letters* 9.12 (Dec. 1966), pp. 425–427. ISSN: 0003-6951. DOI: 10.1063/1.1754639.

[18] R. T. Beyer. "10 - Nonlinear Acoustics". In: *Properties of Polymers and Nonlinear Acoustics*. Ed. by W. P. Mason. Vol. 2. Physical Acoustics. Academic Press, 1965, pp. 231–264. DOI: https://doi.org/10.1016/B978-0-12-395662-0.50014-X.

[19] A. Korpel and R. Adler. "Parametric phenomena observed on ultrasonic waves in water". In: *Applied Physics Letters* 7.4 (Aug. 1965), pp. 106–108. ISSN: 1077-3118. DOI: 10.1063/1.1754311.

[20] L. Adler and M. Breazeale. "Excitation of subharmonics in a resonant ultrasonic wave system". In: *Die Naturwissenschaften* 55.8 (1968), pp. 385–385. DOI: 10.1007/BF00593285.

[21] L. Adler and M. A. Breazeale. "Generation of Fractional Harmonics in a Resonant Ultrasonic Wave System". In: *The Journal of the Acoustical Society of America* 48.5B (Nov. 1970), pp. 1077–1083. ISSN: 0001-4966. DOI: 10.1121/1.1912245.

[22] J. H. Cantrell, L. Adler, and W. T. Yost. "Subharmonic generation, chaos, and subharmonic resurrection in an acoustically driven fluid-filled cavity". In: *Chaos: An Interdisciplinary Journal of Nonlinear Science* 25.2 (Feb. 2015), p. 023115. ISSN: 1089-7682. DOI: 10.1063/1.4913521.